A responsivity-based criterion for accurate calibration of FTIR emission spectra: identification of in-band low-responsivity wavenumbers

Penny M. Rowe,[1,*] Steven P. Neshyba,[2] Christopher J. Cox,[1] and Von P. Walden[1]

[1]*Department of Geography, University of Idaho, 875 Perimeter Drive, Moscow, Idaho 83843, USA*
[2]*Department of Chemistry, University of Puget Sound, 1500 N. Warner, Tacoma, Washington 98416, USA*
**prowe@harbornet.com*

Abstract: Spectra measured by remote-sensing Fourier transform infrared spectrometers are often calibrated using two calibration sources. At wavenumbers where the absorption coefficient is large, air within the optical path of the instrument can absorb most calibration-source signal, resulting in extreme errors. In this paper, a criterion in terms of the instrument responsivity is used to identify such wavenumbers within the instrument bandwidth of two remote-sensing Fourier transform infrared spectrometers. Wavenumbers identified by the criterion are found to be correlated with strong absorption line-centers of water vapor. Advantages of using a responsivity-based criterion are demonstrated.

OCIS codes: (120.0280) Remote sensing and sensors; (120.3180) Interferometry; (120.5630 Radiometry; (120.6200) Spectrometers and spectroscopic instrumentation; (280.4991) Passive remote sensing.

References and links

1. R. O. Knuteson, H. E. Revercomb, F. A. Best, N. C. Ciganovich, R. G. Dedecker, T. P. Dirkx, S. C. Ellington, W. F. Feltz, R. K. Garcia, H. B. Howell, W. L. Smith, J. F. Short, and D. C. Tobin, "Atmospheric emitted radiance interferometer. Part I: instrument design," J. Atmos. Ocean. Technol. 21(12), 1763–1776 (2004a).
2. H. E. Revercomb, H. Buijs, H. B. Howell, D. D. Laporte, W. L. Smith, and L. A. Sromovsky, "Radiometric calibration of IR Fourier transform spectrometers: solution to a problem with the high-resolution interferometer sounder," Appl. Opt. 27(15), 3210–3218 (1988).
3. L. A. Sromovsky, "Radiometric errors in complex Fourier transform spectrometry," Appl. Opt. 42(10), 1779–1787 (2003).
4. P. M. Rowe, S. P. Neshyba, and V. P. Walden, "A responsivity-based criterion for accurate calibration of FTIR emission spectra: theoretical development and bandwidth estimation," Opt. Express 19(6) 5451-5463 (2011)
5. G. Lesins, L. Bourdages, T. Duck, J. Drummond, E. Eloranta, and V. Walden, "Large surface radiative forcing from topographic blowing snow residuals measured in the high arctic at eureka," Atmos. Chem. Phys. 9(6), 1847–1862 (2009).
6. A. Shimota, H. Kobayashi, and S. Kadokura, "radiometric calibration for the airborne interferometric monitor for greenhouse gases simulator," Appl. Opt. 38(3), 571–576 (1999).
7. P. J. Minnett, R. O. Knuteson, F. A. Best, B. J. Osborne, J. A. Hanafin, and O. B. Brown, "the marine-atmospheric emitted radiance interferometer: a high-accuracy, seagoing infrared spectroradiometer," J. Atmos. Ocean. Technol. 18(6), 994–1013 (2001).
8. S. Chandrasekhar, *Radiative Transfer*. (Dover, 1960).
9. L. S. Rothman, D. Jacquemart, A. Barbe, D. Chrisbenner, M. Birk, L. Brown, M. Carleer, C. Chackerianjr, K. Chance, and L. Coudert, "The 2004 molecular spectroscopic database," J. Quant. Spectrosc. Radiat. Transf. 96(2), 139–204 (2005).
10. S. A. Clough, M. W. Shephard, E. J. Mlawer, J. S. Delamere, M. J. Iacono, K. Cady-Pereira, S. Boukabara, and P. D. Brown, "Atmospheric radiative transfer modeling: a summary of the AER codes," J. Quant. Spectrosc. Radiat. Transf. 91(2), 233–244 (2005).
11. R. Knuteson, Cooperative Institute for Meteorological Satellite Studies – SSEC, University of Wisconsin-Madison, 1225 W. Dayton St., Madison, WI 53706 (personal communication, 2010).
12. R. O. Knuteson, H. E. Revercomb, F. A. Best, N. C. Ciganovich, R. G. Dedecker, T. P. Dirkx, S. C. Ellington, W. F. Feltz, R. K. Garcia, H. B. Howell, W. L. Smith, J. F. Short, and D. C. Tobin, "Atmospheric emitted radiance interferometer. Part II: instrument performance," J. Atmos. Ocean. Technol. 21(12), 1777–1789 (2004b).

#138323 - $15.00 USD Received 18 Nov 2010; revised 25 Feb 2011; accepted 8 Mar 2011; published 16 Mar 2011

13. P. Rowe, L. Miloshevich, D. Turner, and V. Walden, "Dry bias in Vaisala RS90 radiosonde humidity profiles over antarctica," J. Atmos. Ocean. Technol. 25(9), 1529–1541 (2008).
14. Data from the AERI operated at the North Slope of Alaska is available at *http://www.archive.arm.gov*.

1. Introduction

Atmospheric infrared radiation is routinely measured using Fourier transform infrared (FTIR) spectrometers [1]. Raw measurement spectra are calibrated using spectra of hot and cold calibration sources of known emission (e.g [2]). The variance of a calibrated spectrum due to noise in raw spectra can be expressed analytically if approximations are made that are valid in the limit of low noise [3]. Outside the low-noise limit, however, the variance must be calculated numerically as described in a companion paper by three of the authors (Rowe, Neshyba, and Walden [4]; hereafter RNW). RNW present a general expression for the variance (that is, for any noise level), showing that it is (formally) infinite. The variance can be approximated as finite in the limit of low noise, or more precisely, when the uncertainty in the measurement of the instrument responsivity (σ_r) divided by the true system responsivity (r) is small ($\sigma_r/r<<1$). However, outside the low-noise limit, the infinite variance corresponds to arbitrarily large noise spikes in calibrated radiances. Furthermore, within the low-noise limit, errors in the calibrated radiance due to random noise in raw spectra are also random, but outside this limit errors are not generally random. Instead, large noise causes a bias in calibrated radiances. For these reasons, it is important to set a criterion for accurate calibration. The criterion $\sigma_r/r<0.3$ was shown by RNW to result in a negligible bias and a variance for 99.999% of measurements that agrees with the low-noise approximation to within 20%.

As an application of the criterion, RNW calculated σ_r/r for upwelling and downwelling FTIR measurements to assess whether the condition $\sigma_r/r < 0.3$ is met within the bandwidth specified. For an Atmospheric Emitted Radiance Interferometer (AERI) operated at Eureka, Canada [5], σ_r/r was found to be generally less than 0.3 within the specified bandwidth, indicating that most in-band radiances are accurately calibrated. However, σ_r/r was found to be greater than 0.3 at particular wavenumbers within the instrument's specified bandwidth, where r was small. At the same wavenumbers, extremely large errors were sometimes observed in calibrated spectra. For example, on 1 July 2008 errors were as large as 2800 RU [radiance unit; 1 RU = 1 mW m^{-2} sr^{-1} $(cm^{-1})^{-1}$]. Such large errors correspond to spectral features in raw uncalibrated spectra that have been attributed to absorption by CO_2 and H_2O inside the instrument [2]. At these wavenumbers, the absorption coefficients of CO_2 and H_2O are strong enough to absorb almost all of the calibration-source radiation, making accurate calibration impossible. This problem only occurs when air is present inside the instrument and thus is not observed in space-borne instrumentation, such as the Interferometric Monitor for Greenhouse Gases (IMG [4,6]).

Identifying measured radiances with large errors and replacing them with reasonable values is particularly important since further processing involving Fourier transforms (e.g. correcting the instrument's finite field of view and "zero-padding" the spectrum onto a standard wavenumber grid) can cause the error to "ring" into radiances at neighboring wavenumbers.

In this work, we suggest using a criterion in terms of σ_r/r to identify wavenumbers where absorption by trace gases within the instrument prevents accurate calibration. Because the responsivity is low at such wavenumbers, as will be shown, we refer to these hereafter as "low-responsivity wavenumbers." In current AERI processing software [7], quality control includes identification of large spikes in calibrated radiances using a criterion we term the "ratio criterion." Both the responsivity criterion and the ratio criterion are applied to measurements made with AERI instruments to show that the responsivity criterion is better suited for identifying low-responsivity wavenumbers and is widely applicable to FTIR spectrometers. We suggest replacing radiances at wavenumbers where $\sigma_r/r > 0.3$, based on the work of RNW, but this threshold can be modified as needed for specific instruments and experiments. Wavenumbers are identified over a 21-month field season using an AERI at

#138323 - $15.00 USD Received 18 Nov 2010; revised 25 Feb 2011; accepted 8 Mar 2011; published 16 Mar 2011

Eureka, Canada, and the likelihood of identification is compared to the strength of the water-vapor absorption coefficient.

The organization of the paper is as follows. In section 2, we give a theoretical overview, first showing that the transmission of air inside the instrument's optical path is implicitly included in the instrument responsivity. We then summarize the theoretical development of RNW, in which expressions for the variance and bias in a calibrated radiance, valid at all noise levels, were derived. In section 3, we describe the ratio criterion for identifying highly erroneous radiances and apply both the ratio criterion and the responsivity criterion to measured AERI spectra. We also argue that radiances at identified wavenumbers should be replaced with surrogates based on the ambient surface temperature, in contrast to existing practice. Finally, we suggest a method to avoid biases that occur when corrected radiances are averaged, showing that the method is well suited for the responsivity criterion. Section 4 presents conclusions.

2. Theoretical overview

The calibrated spectral radiance of a scene is given by Revercomb et al. [2] as

$$L_s + \varepsilon_L = \mathrm{Re}\left[\frac{V_s - V_c}{V_h - V_c}\right]\left[L_h - L_c\right] + L_c, \tag{1}$$

where we have explicitly included the error in L_s due to noise, ε_L, and where V_s, V_h and V_c are raw spectra of the scene and hot and cold calibration source of known radiances, L_h and L_c. Re represents taking the real part, and all terms are functions of wavenumber. At wavenumbers where the absorption coefficient of a trace gas is large, we expect most scene radiation to originate from near the instrument. If the cold calibration source is kept at ambient temperature, then, at these wavenumbers, in the absence of errors, $V_s - V_c = 0$, and $L_s = L_c$. However, if air is present within the instrument, the absorption coefficients of CO_2 and H_2O can be so large that these trace gases absorb and re-emit almost all calibration-source radiation, so that $V_h = V_c$, and the denominator in Eq. (1) approaches zero. In this section, we first show that the transmission of air inside the instrument is included implicitly in the instrument responsivity, r, so that identifying wavenumbers where the instrument does not transmit enough source radiation for accurate calibration can be accomplished with a criterion in terms of σ_r/r. Following this, we summarize the work of RNW, showing the effect of large σ_r/r on the variance and bias of calibrated spectra.

2.1 Transmission of air inside the instrument

The equation of radiative transfer through an atmosphere in the absence of scattering and in local thermodynamic equilibrium is

$$I(z) = I(z_0)t(z_0, z) + \int_{z_0}^{z} \mathrm{B}\left(T(z')\right)\left[\frac{dt(z', z)}{dz'}\right]dz' \tag{2}$$

[8], where z' is position, $I(z_0)$ is the source radiation, t is transmittance, and B is the Planck function at temperature T. The parenthesis in Eq. (2) represent functionality. I, t, and B are functions of wavenumber as well as position. For FTIR spectrometers, this equation governs the transfer of radiation through the air inside the instrument, that is, from the calibration source at position z_0 to the detector at position z. For the view of the hot calibration source, $I(z_0)$ is L_h and for the cold calibration source, $I(z_0)$ is L_c. The transmittance $t(z_0,z)$ is the transmittance through the air inside the instrument; we define $t_{AI} \equiv t(z_0,z)$. The integral term in Eq. (2) represents the radiance contribution from within the instrument, given the symbol O. Thus the radiation transferred from the hot calibration source through the air inside the instrument is $L_h t_{AI} + O$.

#138323 - $15.00 USD Received 18 Nov 2010; revised 25 Feb 2011; accepted 8 Mar 2011; published 16 Mar 2011

The signal measured by the detector also depends on the overall system efficiency, η, the instrument phase, ϕ, and the detector response, R_d. Including these terms as dictated by Sromovsky [3], the signal measured when viewing the hot calibration source is given by

$$V'_h = 0.5\eta R_d t_{Al} L_h \exp(i\phi) + R_d O, \tag{3}$$

where this equation differs from Eq. (18) of Sromovsky [3] in two respects: the prime on V_h indicates that errors are not taken into account, and the transmittance term t_{Al} is included here (but is not in [3]). As pointed out by Sromovsky (first paragraph of section 6C of [3]) a term needs to be added to account for error. We express the error as $n_h \exp(i\phi)$ instead of $R_d \eta/2\ \varepsilon_x$ (as in [3]), for reasons given in RNW, so that

$$V_h = 0.5\eta R_d t_{Al} L_h \exp(i\phi) + R_d O + n_h \exp(i\phi). \tag{4}$$

For views of the cold calibration source and sky, subscripts h are replaced with subcripts c and s, respectively.

Sromovsky defines the system responsivity, r, to be the proportionality constant $0.5\eta R_d$. In the present treatment, we show that r also includes t_{Al}. Since the detector response and optical efficiency vary slowly with wavenumber [2], fine spectral structure in the instrument responsivity is expected to be due to t_{Al}.

The system responsivity can be estimated from measurements as

$$r_m \equiv (V_h - V_c)/(L_h - L_c) \tag{5}$$

(as in [2], but note that we have not taken the magnitude of the right hand side). The standard deviation of r_m, σ_r, can be estimated from sequential measurements of r_m or from knowledge of the statistical properties of n_h and n_c, since $\sigma_r^2 = \left\langle \|e_r\|^2 \right\rangle$ (RNW), where the brackets indicate the mean and the double bars indicate the magnitude, and where $e_r \equiv (n_h - n_c)/(L_h - L_c)$ (ignoring variations in L_h, L_c, ϕ and O).

Figure 1 shows $\|r_m\|$ and an estimate of t_{Al} for an AERI operated at Eureka, Canada. The transmittance was calculated using absorption coefficients from the HITRAN database [9] as input into the Line By Line Radiative Transfer Model (LBLRTM v. 10.3 [10]) for a 1 meter path, a temperature of 283 K, and 100% relative humidity. The transmittance and the responsivity both vary slowly with wavenumber for much of the spectrum, but drop precipitously at the center of the strong CO_2 band at 667 cm^{-1} and at the centers of strong lines in the ν_2 band of water vapor (1300 to 1900 cm^{-1}; circles). As discussed below, wavenumbers where r falls below the threshold $3\sigma_r$ (also shown in the figure) should be rejected as corresponding to calibrated radiances having errors that may be arbitrarily large. Since r is proportional to t_{Al}, r will decrease with t_{Al} as the humidity increases. Thus we expect to identify more wavenumbers for rejection in warmer, wetter ambient conditions.

2.2 Variance and bias of calibrated spectra

Here we briefly review the theoretical development of RNW, leading to expressions for the variance and bias in a calibrated radiance, expressed in terms of σ_r/r, which are valid for any noise level. As shown in RNW, error in the calibration radiance is

$$\varepsilon_L = (sf_s - f_c)(L_h - L_c) + (f_r)(L_c - L_s), \tag{6}$$

where f_s, f_c, and f_r are given by replacing the subscript x with subscripts s, c, or r in

$$f_x \equiv \mathrm{Re}\left[\frac{e_x / r}{1 + (e_r / r)}\right], \tag{7}$$

and where $e_c \equiv n_c/(L_h - L_c)$ and $e_s \equiv (n_s/s)/(L_h - L_c)$, by analogy with e_r.

#138323 - $15.00 USD Received 18 Nov 2010; revised 25 Feb 2011; accepted 8 Mar 2011; published 16 Mar 2011

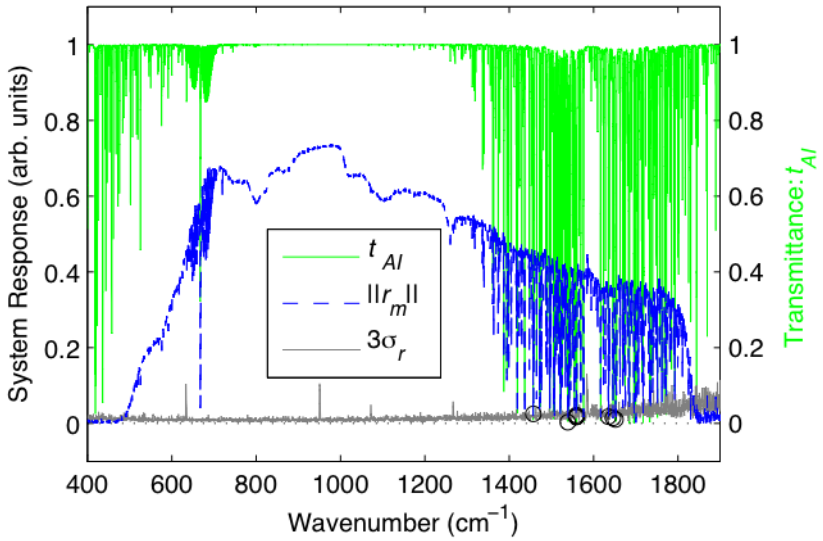

Fig. 1. Estimate of system responsivity ($||r_m||$) and the standard deviation of r_m (σ_r) for an Atmospheric Emitted Radiance Interferometer (AERI), and an estimate of the transmittance of air through the instrument (t_{AI}). Circles indicate points with large errors.

Furthermore, the factor s before f_s in Eq. (6) is defined such that n_s/s has the same standard deviation as n_h (as noted in RNW, we have assumed that the standard deviations of n_h and n_c are the same, but that the standard deviation of n_s may differ due to acquiring raw spectra with different numbers of spectral averages, or coadditions).

In the low-noise limit that $e_r/r << 1$, $<\varepsilon_L> = 0$, and thus the variance ($<\varepsilon_L^2>$-$<\varepsilon_L>^2$) is $<\varepsilon_L^2>$. Sromovsky shows that the variance in the low-noise limit is (in the notation of RNW)

$$\left\langle \varepsilon_L^2 \right\rangle \approx \frac{\sigma_{n_s}^2}{r^2} + \left(\frac{\sigma_{n_c}^2}{r^2}\right)\left(\frac{L_h - L_s}{L_h - L_c}\right)^2 + \left(\frac{\sigma_{n_h}^2}{r^2}\right)\left(\frac{L_c - L_s}{L_h - L_c}\right)^2. \quad (8)$$

A more general expression for $<\varepsilon_L^2>$ is derived in RNW, given as

$$\left\langle \varepsilon_L^2 \right\rangle = \left(s^2 \left\langle f_s^2 \right\rangle + \left\langle f_c^2 \right\rangle\right)\left(L_h - L_c\right)^2 + \left\langle f_r^2 \right\rangle \left(L_c - L_s\right)^2 - 2\left\langle f_c f_r \right\rangle \left(L_h - L_c\right)\left(L_c - L_s\right), \quad (9)$$

Reviewing Eq. (7), we see that the f^2 terms in Eq. (9) approach infinity as e_r/r approaches -1. Although the variance is thus formally infinite, for $\sigma_r/r << 1$, $|\, e_r/r \,|$ is unlikely to ever approach values as large as one, and the variance can be approximated as finite [Eq. (8)]. However, as σ_r/r gets larger, the probability of infinite f^2 increases; this corresponds to a probability of arbitrarily large errors in calibrated radiances.

Outside the low-noise limit, RNW find that $<\varepsilon_L> \neq 0$, but rather,

$$L_s + \left\langle \varepsilon_L \right\rangle = 0.5 \left\langle f_r \right\rangle \left(L_h + L_c\right). \quad (10)$$

In RNW, $<f_r>$ is calculated numerically and found to vary from 0 to 1 as σ_r/r increases from 0 to infinity (see Fig. 2 of RNW). Figure 3 of RNW shows that averages of calibrated radiances approach $0.5(L_h + L_c)$ outside the instrument bandwidth and at specific points in-band, where σ_r/r is very large.

In RNW, numerical calculations were used to determine that the threshold $\sigma_r/r \leq 0.3$ corresponds to a bias [$\leq \sim 10^{-5}(L_h + L_c)$] that is negligible compared to most error budgets, and a variance for 99.999% of measurements that is within 20% of the variance in the low-noise approximation. This threshold was used to check the bandwidth of an AERI and a satellite-borne instrument.

#138323 - $15.00 USD Received 18 Nov 2010; revised 25 Feb 2011; accepted 8 Mar 2011; published 16 Mar 2011

The opposite condition, $\Gamma_r > 0.3$, can be used to identify calibrated radiances at wavenumbers in-band where absorption by trace gases within the instrument's optical path makes accurate calibration impossible. The remainder of this paper focuses on these in-band wavenumbers for specific instruments.

3. Applications

In this section, we show that the responsivity criterion can accurately identify low-responsivity wavenumbers. To put the responsivity criterion into context, we first discuss a method (termed the "ratio criterion") currently included as quality-control in the standard AERI processing [7], whose purpose is to identify large spikes in calibrated radiances (that lead to ringing when Fourier transforms are performed in further processing). [11] Here, we apply both criteria to measurements from two AERI instruments, one with low noise and one with relatively high noise. We also provide a method for avoiding biases that can occur when corrected radiances are averaged. We then show how Fourier transforms can cause errors to ring into neighboring wavenumbers, making it important to replace radiances that have large errors. Finally, we apply the responsivity criterion to a year-long field experiment at Eureka, Canada, showing that the number of times a given wavenumber is identified correlates well with the strength and proximity of the nearest strong line center in the absorption spectrum of water vapor.

3.1 Case study: low noise

Figure 2a shows the calibrated downwelling radiance measured by an AERI at Eureka, Canada at 0357 UTC on 1 July 2008 [5]. The AERI instrument is described in general by Knuteson et al. [12]. This AERI has a standard detector and is sensitive from about 500 to 1800 cm^{-1}, exhibiting relatively low noise [13]. Absorption features due to CO_2, O_3, and H_2O are labeled in the figure. In the "atmospheric window" from 900 to 1300 cm^{-1}, there is little emission from trace gases, except O_3. At the center of the CO_2 band (667 cm^{-1}) and in the ν_2 band of water vapor (1300 to 1900 cm^{-1}), the absorption coefficient can be strong enough that almost all source radiation is absorbed and re-emitted within the optical path of the instrument. A few radiances in the water-vapor ν_2 band having large errors (≥10 RU) are indicated (circles); these correspond to the extremely low responsivities indicated previously in Fig. 1. Since the emission is known to be strong at these wavenumbers, we expect that if accurate calibration were possible, then L_s would be ≈B(T_a), where B indicates the Planck function and T_a is the ambient temperature. An estimate of B(T_a) is shown on the figure, derived from the radiance observed between 672 and 682 cm^{-1}, a region known to saturate close to (but outside) the instrument. Also shown is the Planck function of the temperature of the cold calibration blackbody, B(T_c), which is (approximately) the radiance emitted by the cold calibration-source. B(T_c) is greater than B(T_a) because the cold calibration source was warmed to slightly above-ambient temperatures.

The ratio criterion identifies wavenumbers where the real part of the ratio of uncalibrated spectral differences, Re[(V_s-V_c)/(V_h-V_c)], falls outside a set of pre-determined bounds. The bounds are intended to be generous enough to filter out large spikes in calibrated radiances but not noisy data generally, and to be widely applicable geographically and with variations in instruments [11]. However, the uncalibrated sky spectrum (V_s) is highly variable both spectrally and with atmospheric conditions. Figure 2b demonstrates how the ratio criterion is applied. A set of bounds is chosen, in this case at +1.5 and −1.5 (red dashed lines). The ratio is calculated for each scene spectrum. The blue curve in the figure indicates the ratio for the case study on 1 July 2008 at 3.94 UTC. Wavenumbers are identified where Re[(V_s-V_c)/(V_h-V_c)] > 1.5 or Re[(V_s-V_c)/(V_h-V_c)] < −1.5. For this case, a single point is identified above 1.5, while many points are identified below −1.5. In current AERI processing, calibrated radiances at these wavenumbers are then replaced with the radiance from the cold calibration source, B_c. Over the course of the day, the ratio will change slightly at most wavenumbers as V_s changes with atmospheric conditions and V_c changes with the temperature of the cold calibration-

#138323 - $15.00 USD Received 18 Nov 2010; revised 25 Feb 2011; accepted 8 Mar 2011; published 16 Mar 2011

source (V_h is generally constant because the hot calibration-source is generally maintained at a constant temperature). At low-responsivity wavenumbers, the ratio will change dramatically with noise fluctuations, causing different ratio values to fall outside the bounds and be identified.

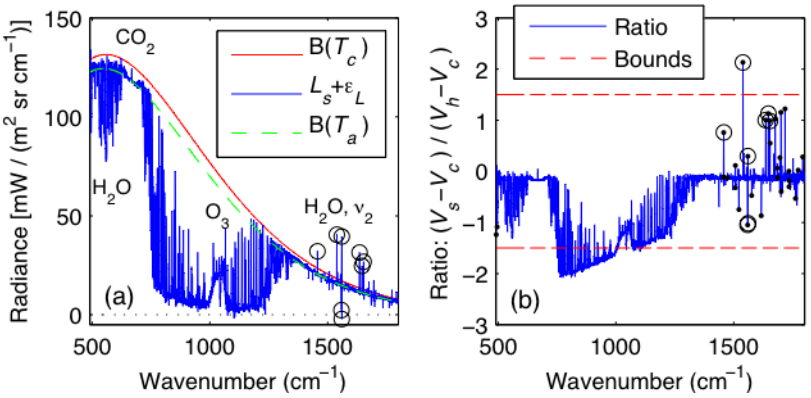

Fig. 2. a) The calibrated downwelling radiance (L_s + ε_L) measured with an Atmospheric Emitted Radiance Interferometer (AERI) at Eureka, Canada on 1 July 2008 at 0357 UTC, and the Planck functions of the temperature of the cold calibration-source, B(T_c), and ambient temperature, B(T_a). A few radiances having significant errors are circled. b) The real part of the ratio of uncalibrated difference spectra for the measurement shown in a). Bounds used to identify spectral data points with large errors are shown. Dots indicate points identified with a criterion in terms of the relative error in the instrument responsivity, σ_r/r.

Wavenumbers identified as corresponding to high radiance errors and low responsivity in Fig. 2a (circles) are also circled in Fig. 2b. Of these wavenumbers, only one is identified by the ratio criterion. Furthermore, most wavenumbers between 800 and 1000 cm^{-1} are incorrectly identified as having large errors because most ratio values fall below the lower bound (–1.5). At these wavenumbers, replacing the calibrated radiance with L_c would result in errors of up to 100 RU (as evident in Fig. 2a). The ratio values fall outside the bounds not because of radiance errors, but rather because the bounds were set for a warmer location, where V_s is larger in the atmospheric window. V_s changes with geographic location, season, the diurnal cycle, and weather conditions. The lower bound needs to be reduced so these wavenumbers are not identified. Thus the ratio criterion, designed to identify large error spikes in V_s, is not well-suited to identify low-responsivity wavenumbers since the bounds are largely determined by the variability in V_s, rather than the responsivity.

To identify wavenumbers using the responsivity criterion, σ_r/r was calculated for this case study. Since instrument temperatures and the instrument phase were fairly stable with time, σ_r was calculated as the standard deviation of 20 sequential measurements of r_m taken over about 15 minutes, and r was estimated as $\|<r_m>\|$. The criterion that $\sigma_r/r > 0.3$ was then used to identify low-responsivity wavenumbers.

In contrast to the ratio criterion, the responsivity criterion identified all but one of the circled points, in addition to 21 others (points identified using the responsivity criterion are shown in Fig. 2b as small black dots). Visual examination confirms that at many of the wavenumbers identified by the responsivity criterion there are noise spikes in the ratio. At a few wavenumbers identified there do not appear to be noise spikes. This is not surprising, since the criterion for selection is not based on knowledge that errors are large, but rather on the likelihood that errors might be arbitrarily large. Since these wavenumbers are all near the centers of extremely strong lines in the water-vapor absorption coefficient, the true radiance is known to be close to the Planck function of ambient temperature [B(T_a) in Fig. 2a], so replacing measured radiances with B(T_a) will not cause large errors.

The responsivity criterion has several advantages for identifying low-responsivity wavenumbers. It accurately identifies low-responsivity wavenumbers if the humidity at the

#138323 - $15.00 USD Received 18 Nov 2010; revised 25 Feb 2011; accepted 8 Mar 2011; published 16 Mar 2011

surface changes, without adjusting any parameters, since there will be a corresponding decrease in r. It is not affected by atmospheric conditions above the surface, since r does not depend on V_s. Furthermore, the threshold for σ_r/r is associated with a bias magnitude and variance that have been quantified by RNW. Thus the threshold can be set to achieve the desired statistics (RNW recommend a threshold of 0.3) regardless of atmospheric conditions.

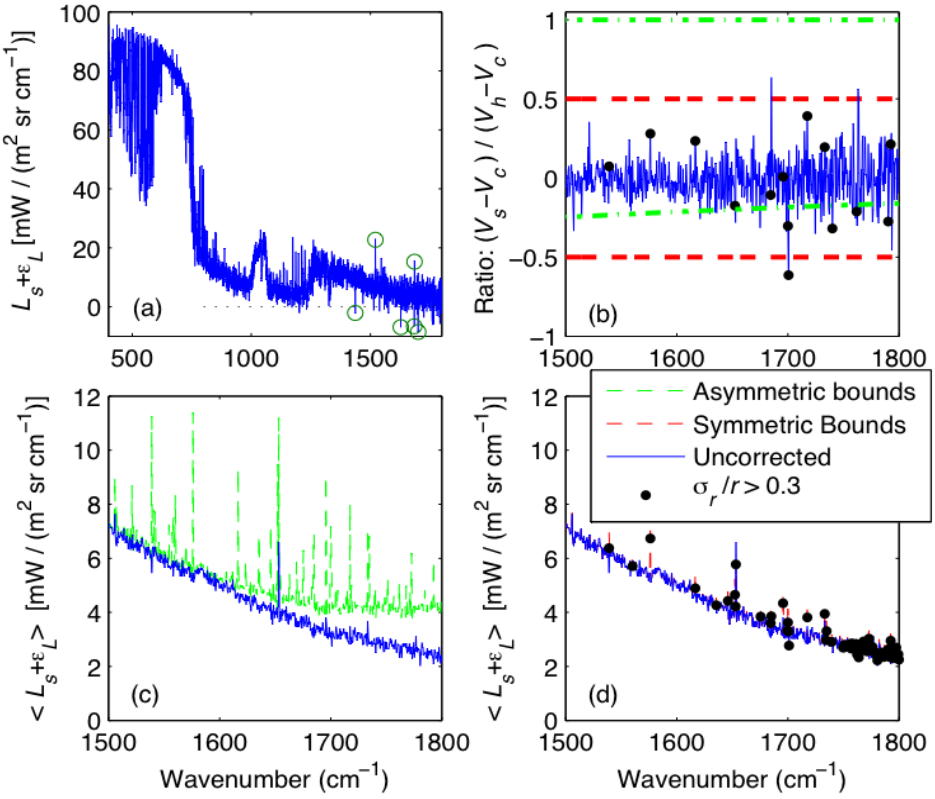

Fig. 3. a) The calibrated downwelling sky radiance (L_s+ε_L) measured with an Atmospheric Emitted Radiance Interferometer (AERI) at the North Slope of Alaska at 0102 UTC on 1 Feb. 2010. Radiances appearing to have large errors are circled. b) The corresponding ratio of uncalibrated difference spectra as well as symmetric and asymmetric bounds used in quality control and points identified using a responsivity criterion (dots). c) The average of calibrated radiances measured over the course of the day (<L_s+ε_L>, blue) and the average of spectra corrected using the asymmetric bounds (green dashed). d) <L_s+ε_L> (blue) and the averages of spectra corrected using symmetric bounds (red dashed) and the responsivity criterion (dots).

3.2 Case study: high noise

Figure 3a shows an AERI measurement made at the North Slope of Alaska (NSA) Atmospheric Radiation Measurement (ARM) site, near Barrow, Alaska, at 0102 UTC on 1 February 2010, when a thin cloud was overhead. The NSA AERI uses a detector that is sensitive at longer wavelengths than the AERI at Eureka (i.e. below 500 cm^{-1}), but has much larger detector noise from 500 to 1800 cm^{-1} [14]. A few radiances with large errors at low-responsivity wavenumbers are circled; these are less readily apparent in this figure due to the higher level of instrument noise than for the instrument used at Eureka. As shown in this subsection, identification of low-responsivity wavenumbers becomes more challenging when noise is high. In addition, it is shown that correction methods based on both the ratio criterion and the responsivity criterion can introduce biases in averages of corrected calibrated radiances; a simple procedure to avoid these biases is suggested.

#138323 - $15.00 USD Received 18 Nov 2010; revised 25 Feb 2011; accepted 8 Mar 2011; published 16 Mar 2011

In addition to asymmetric bounds, Fig. 3b also shows a set of symmetric bounds (at ±0.5) developed especially for this case study. These bounds are only used to identify wavenumbers from 1500 to 1800 cm^{-1}. Figure 3d (red dashed line) shows the average of calibrated radiances after replacing radiances at wavenumbers where the ratio falls outside the symmetric bounds. We see that using symmetric bounds eliminates most of the bias (the plot of the average of uncorrected spectra falls directly on top of the red dashed line). However, at a few wavenumbers the red dashed line differs from the average of uncorrected spectra. Thus, even bounds that are symmetric about zero can induce biases at particular wavenumbers. To avoid biases the bounds need to be symmetric not about zero, but about the value the ratio would have in the absence of errors. The ratio is only expected to be zero when $V_s = V_c$, which in turn occurs only near strong line centers when $T_a \approx T_c$. On this day, T_c lagged T_a and was on average 1.2 K colder, making the ratio slightly negative near strong line centers, so that negative errors were more likely to be identified.

Low-responsivity wavenumbers were also identified using the responsivity criterion. To estimate r and σ_r, the average and standard deviation of 20 sequential measurements of r_m were used (taken before, during, and after the spectrum of interest). For each spectrum, radiances were replaced at wavenumbers where $\sigma_r/r > 0.3$. For example, black dots in Fig. 3b indicate ratio values for which $\sigma_r/r > 0.3$ at 0102 UTC. As for the ratio criterion, the corrected radiances for the full day were averaged. Slightly different wavenumbers were identified for each spectrum so that over the course of the day 66 wavenumbers were identified at least once (Fig. 3d, which thus has more dots than for the single case shown in Fig. 3b). Many of the wavenumbers identified (43) fall between 1750 and 1800 cm^{-1}, where the instrument is less sensitive. The black dots shown in Fig. 3d indicate not only the wavenumbers identified, but also the averages of the corrected radiances. Comparing this average to the average of uncorrected spectra, we see that correcting spectra using the responsivity criterion can also cause biases in averaged spectra. These biases are smaller than when wavenumbers are identified using the ratio with bounds of ±0.5 and occur at fewer wavenumbers. The bias occurs because wavenumbers where the errors in r_m are negative (n_h-$n_c < 0$) are more likely to be identified than errors that are positive, since negative errors reduce r_m, bringing it closer to the threshold σ_r. The bias is mitigated by averaging r_m to decrease noise in the estimate of r.

To avoid biases in averaged calibrated radiances, we suggest a simple procedure. For the time period chosen for averaging, the lists of wavenumbers identified for each spectrum should be combined. Radiances should then be replaced in all spectra at all wavenumbers identified over the entire time period. A responsivity criterion is better suited than a ratio criterion for implementing this procedure for the following reasons. If noise is large, occasionally errors in calibrated spectra will be large enough to be identified by the ratio criterion. However, as long as errors are random, they will average out, and replacing these radiances is not needed. Indeed, accurate radiance-averages may be replaced with incorrect values if the responsivity is not low (i.e. if the radiance does not originate from close to the instrument). Thus the goal is not to identify large random errors, but rather to identify wavenumbers where errors are systematic. As discussed by RNW, high noise and/or low responsivity cause systematic errors in calibrated spectra. Thus a criterion in terms σ_r/r is best suited to identify wavenumbers where averaged radiances are inaccurate.

3.3 Ringing

If radiances at low-responsivity wavenumbers are not replaced with reasonable values, further processing may corrupt results at neighboring wavenumbers. For example, correction of the instrument lineshape for the effects of the instrument's finite field of view and resampling the spectrum onto a standard wavenumber grid both involve taking the fast Fourier transform (FFT) and inverse FFT (IFFT), causing error to "ring" into neighboring wavenumbers and corrupting them as well. If the error is moderate, the ringing may be acceptable compared to other errors. For example, a noise spike of 40 RU results in error due to ringing of 0.6 RU approximately 2 wavenumbers from the spike. However, larger errors lead to unacceptable corruption of nearby wavenumbers. Figure 4 shows the ringing due to resampling onto a

#138323 - $15.00 USD Received 18 Nov 2010; revised 25 Feb 2011; accepted 8 Mar 2011; published 16 Mar 2011

standard wavenumber grid by zero-filling (taking the IFFT, zero-padding, and taking the FFT) for an AERI measurement at Eureka at 0648 UTC on 1 July 2008. The plot was enlarged to show the ringing about a noise spike of 1410 RU (the noise spike falls outside the upper plot boundary). The dashed curve shows the original radiance without resampling, the solid curve shows the radiance after resampling if the noise spike is not corrected, and the red dots show the radiance after resampling if the noise spike is replaced with the radiance shown at 1521 cm^{-1}. If the erroneous point is not replaced with a reasonable value, the error due to ringing is still 4 RU as far as ±10 wavenumbers from the line center.

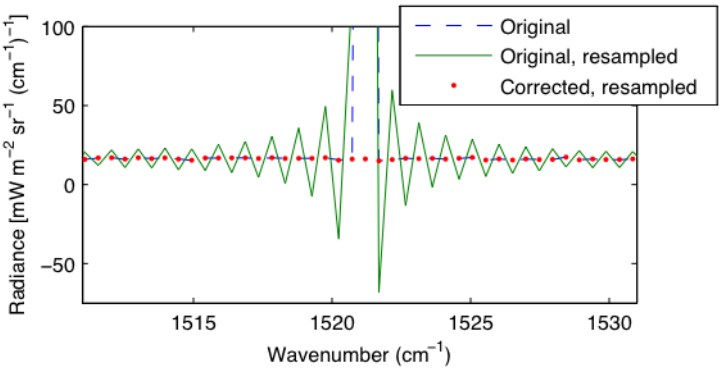

Fig. 4. An expanded region of a downwelling radiance spectrum centered on the strong water-vapor absorption line at 1521.3 cm^{-1}, where an error of 1410 RU occurs (blue dashed curve; the error is outside the plot limits). Resampling using Fourier transforms causes the error to "ring" into neighboring wavenumbers (green solid line) unless the error is first removed (red dots). This spectrum was obtained at Eureka, Canada at 0648 UTC on 1 July 2008.

To reduce errors due to ringing as much as possible, it is important to replace radiances with the best estimate possible. Since the problem occurs because absorption and emission is so strong that most radiance originates from within the instrument, we know that if air were not present in the instrument, most radiance would originate from only a short distance away. Thus the radiance should be close to that of a blackbody at ambient temperature (T_a). If the temperature of the cold calibration source (T_c) is very close to T_a, it is convenient to replace erroneous radiances with the (known) cold calibration-source radiance. However, the temperature of the cold calibration source is sometimW 4es different than ambient temperature. The temperature of the cold calibration source often lags ambient temperature and, in cold conditions the cold source may be heated slightly to prevent the formation of frost on its surface. For example, in one case the cold blackbody temperature and the ambient temperature differed by 2.4K, corresponding to a radiance difference of 1 RU at 1600 cm^{-1}. Instead of using T_c, T_a can be estimated from the brightness temperature between 672 and 682 cm^{-1}, a region known to saturate close to (but outside) the instrument.

We suggest that the responsivity criterion be used to identify low-responsivity wavenumbers, so that erroneous radiances can be replaced.

3.4 Field season

Wavenumbers where $\sigma_r/r > \sim 0.3$ were identified for AERI spectra measured at Eureka, Canada for a 21-month field season, from March 2006 to December 2007. Because σ_r is relatively low for this data set, it is relatively easy to identify points where $r \sim 0$, due to the dramatic difference seen in σ_r/r at these points. Thus both σ_r and r were calculated very roughly, as follows. It was assumed that the noise was low enough that r could be approximated as $||r_m||$ for each measurement (i.e. averaging sequential values of r_m was unnecessary). To estimate σ_r, the standard deviation of r_m with wavenumber was calculated in regions where the instrument is not sensitive (between 400 and 460 cm^{-1} and between 1845

#138323 - $15.00 USD Received 18 Nov 2010; revised 25 Feb 2011; accepted 8 Mar 2011; published 16 Mar 2011

and 1920 cm^{-1}) and a linear variation across the spectrum was assumed. (A more accurate approach would take into account that σ_r is proportional to $1/[L_h - L_c]$).

The most commonly identified wavenumbers for 934,544 spectra measured using the channel 1 detector (500-1800 cm^{-1}) are shown in Table 1 (excluding wavenumbers near the center of the CO_2 band at 667 cm^{-1}). The columns of the table show the frequency with which the wavenumbers were identified (as a percentage of all spectra) and the corresponding wavenumber. Also shown are line strengths and positions of the closest strong water-vapor absorption lines. Line strengths were obtained from the HITRAN database [9]. Columns are ordered by frequency of identification to show the correlation between frequency of identification and line strength; this correlation supports the robustness of the criterion. For example, wavenumbers were identified near all lines having strengths greater than 0.80 x 10^{-19} cm^{-1}/(molecule cm^{-2}). If the humidity increased, the same wavenumbers would be identified, but the frequency of identifications would increase, and additional wavenumbers would be identified. As an alternative to identifying wavenumbers for every spectrum, lists of wavenumbers such as this may be compiled and used for all spectra.

Table 1. Low-Responsivity Wavenumbers Identified for an Atmospheric Emitted Radiance Interferometer (AERI) Operating from April 2006 to December 2007 at Eureka, Canada

N[a] (%)	ν_{obs}[b] (cm^{-1})	ν_0[c] (cm^{-1})	S[d] (SU[1])	N (%)	ν_{obs} (cm^{-1})	ν_0 (cm^{-1})	S (SU)	N (%)	ν_{obs} (cm^{-1})	ν_0 (cm^{-1})	S (SU)
43	1653.3	1653.267	2.42	10	1684.7	1684.835	2.99	0.3	1473.5	1473.514	1.01
41	1695.8	1695.928	2.63	8	1541.9	1542.160	1.10	0.2	1696.2	1695.928	2.63
40	1539.1	1539.061	2.07	8	1734.8	1734.650	1.31	0.1	1772.4	1772.714	1.43
39	1576.2	1576.185	2.59	8	1506.8	1507.058	1.90	0.1	1739.6	1739.839	0.90
37	1652.4	1652.400	2.41	7	1792.7	1792.659	0.97	0.1	1683.2	1683.178	0.67
37	1616.7	1616.711	2.32	6	1652.9	1653.267	2.61	0.1	1522.7	1522.686	0.71
34	1717.5	1717.405	2.09	6	1685.2	1684.835	2.99	0.1	1675.0	1675.173	0.93
31	1700.6	1700.776	0.90	5	1505.8	1505.604	1.90	0.1	1557.9	1557.609	0.58
29	1700.1	1699.934	1.77	2	1472.0	1472.051	1.06	0.1	1768.1	1768.120	0.47
29	1521.2	1521.309	0.85	2	1540.5	1540.300	1.63	0.1	1654.3	1654.511	0.88
28	1436.8	1436.818	1.04	2	1554.5	1554.352	1.29	0.04	1771.5	1771.287	0.48
25	1646.1	1645.969	1.60	2	1734.3	1734.650	1.31	0.04	1663.0	1662.809	0.79
24	1559.8	1560.257	2.17	1	1772.9	1772.714	1.43	0.04	1623.4	1623.559	0.83
23	1635.5	1635.652	1.79	1	1751.2	1751.423	0.86	0.03	1706.4	1706.349	0.50
21	1560.3	1560.257	2.17	0.9	1496.1	1496.249	1.45	0.03	1540.0	1540.300	1.63
18	1675.5	1675.515	0.54	0.8	1558.8	1558.531	2.33	0.03	1636.0	1635.652	1.79
17	1456.6	1456.887	1.69	0.7	1761.8	1761.828	0.76	0.02	1715.0	1715.155	0.69
14	1419.5	1419.508	1.02	0.7	1701.1	1700.776	0.90	0.02	1718.9	1718.612	0.52
13	1733.4	1733.391	1.42	0.6	1569.9	1569.789	0.98	0.01	1718.4	1718.612	0.52
11	1507.2	1507.058	1.90	0.5	1699.6	1669.393	0.96	0.01	1464.8	1464.905	0.88
11	1669.2	1669.393	0.96	0.5	1557.4	1557.486	0.51	0.01	1740.1	1739.839	0.90
10	1558.3	1558.531	2.33	0.3	1635.0	1634.967	0.59	0.01	1704.4	1704.453	0.50
10	1457.1	1456.887	1.69	0.3	1684.2	1683.984	0.47	0.01	1545.3	1545.157	0.79

[a]Identifications, as percent of all spectra measured. [b]The identified wavenumber (ν_{obs}). [c]Position of the strongest line within 0.48 cm^{-1}. [d]Corresponding line strength. [e]SU = 10^{-19} cm^{-1}/(molecule cm^{-2}) at 296K.

4. Conclusions

In a previous paper (RNW [4]), an equation for the variance of the calibrated radiance from FTIR spectrometers, known for low errors, was generalized for all noise levels. In addition, RNW revealed a bias in spectra at high noise levels. A criterion, $\sigma_r/r < 0.3$ (where σ_r/r is the relative error in the system responsivity) was presented for identifying accurately calibrated radiances. This criterion was used to identify the bandwidth of two representative FTIR spectrometers, a ground-based Atmospheric Emitted Radiance Interferometer (AERI) and the satellite-mounted Interferometric Monitor for Greenhouse Gases (IMG).

In this paper we have focused on in-band spectral regions, in an effort to identify wavenumbers that, despite lying inside the nominal band of the instrument, nevertheless cannot be accurately calibrated. Two representative FTIR spectrometers are considered, both ground-based Atmospheric Emitted Radiance Interferometers (AERIs); these spectrometers

#138323 - $15.00 USD Received 18 Nov 2010; revised 25 Feb 2011; accepted 8 Mar 2011; published 16 Mar 2011

differ considerably in the sensitivity of their detectors and therefore afford different opportunities to test the utility of the responsivity-based method developed by RNW. Although most of the in-band spectral region is characterized by high responsivity (hence $\sigma_r/r < 0.3$), we find numerous wavenumbers where the responsivity is low ($\sigma_r/r > 0.3$). We find that the predominant reason for this poor in-band responsivity is absorption by trace gases within the spectrometer, especially water vapor. Errors can be quite large (thousands of RU) and further processing can cause them to corrupt neighboring wavenumbers (for example, errors of 20 to 40 RU result in errors of 0.3 to 0.6 RU approximately 2 wavenumbers away).

A comprehensive comparison of the responsivity-based criterion to currently employed ("ratio criterion") methods for identifying unresponsive wavenumbers is also undertaken. The two methods have different goals: the ratio criterion identifies wavenumbers where errors *happen* to be large in a given spectrum. By contrast, since σ_r is a statistical quantity, it identifies wavenumbers where errors are *likely* to be large. The responsivity criterion is found to be well-suited for identifying low responsivity wavenumbers, since σ_r/r does not depend on the uncalibrated sky spectrum, V_s, but only on instrument characteristics, and should apply in all atmospheric conditions, including the polar regions and lower latitudes. Furthermore, since σ_r is a statistical quantity, the value of σ_r/r corresponds to known error characteristics (i.e. variance and bias, as given in RNW).

We show that both the responsivity criterion and the ratio criterion can induce biases when many corrected spectra are averaged. Biases can be large when asymmetric bounds are used in the ratio method and are expected to be small for bounds that are symmetric and when the responsivity criterion is used. Because such biases occur at identified wavenumbers, a reasonable strategy for avoiding a bias is to combine the lists of identified wavenumbers for the entire averaging period and replace radiances at these wavenumbers in all spectra.

The responsivity criterion is applied to 21 months of AERI spectra at Eureka, Canada, and identified wavenumbers are found to correlate with strong line centers of water vapor. The responsivity criterion is tunable; making the threshold less stringent (increasing it) generally identifies wavenumbers near increasingly weaker lines, while making it more stringent (decreasing it) generally identifies wavenumbers near only the strongest lines.

Acknowledgments

We are grateful to the Canadian Network for the Detection of Atmospheric Change (CANDAC) technicians for operating the AERI instrument at Eureka, Canada from March 2006 through April 2009 and to the Environment Canada Weather Station at Eureka, Nunavut, for their support. We thank the Department of Energy's Atmospheric Radiation Measurement (ARM) program for providing the data for the AERI instrument operating at the North Slope of Alaska (NSA) and Dave Turner for help obtaining the NSA AERI data. We thank Dave Turner and Robert Knuteson for helpful discussions. Support for this research came from the National Aeronautics and Space Administration (NASA) Research Opportunities in Space and Earth Science program (Contract NNX08AF79G), from the National Science Foundation (NSF) Idaho Experimental Program to Stimulate Competitive Research (EPSCoR) and by the NSF under award number EPS-0814387. SPN acknowledges support from the University of Puget Sound.

#138323 - $15.00 USD Received 18 Nov 2010; revised 25 Feb 2011; accepted 8 Mar 2011; published 16 Mar 2011